

Model-Independent Signatures of New Physics in non-Gaussianity

Mark G. Jackson¹ and Koenraad Schalm²

¹*Paris Centre for Cosmological Physics and Laboratoire AstroParticule et Cosmologie, Université Paris 7-Denis Diderot, Bâtiment Condorcet, 10 rue Alice Domon et Léonie Duquet, 75205 Paris, France and*

²*Instituut-Lorentz for Theoretical Physics, University of Leiden, Leiden 2333CA, The Netherlands*

(Dated: September 8, 2018)

We compute the model-independent contributions to the primordial bispectrum and trispectrum in de Sitter space due to high-energy physics. We do this by coupling a light inflaton to an auxiliary heavy field, and then evaluating correlation functions in the Schwinger-Keldysh “in-in” formalism. The high-energy physics produces corrections parametrized by H/M where H is the scale of inflation and M is the mass of the heavy field. The bispectrum peaks near the elongated shape, but otherwise contains no features. The trispectrum receives no corrections at order H/M .

PACS numbers: 04.62.+v, 98.80.-k, 98.70.Vc

INTRODUCTION

The leading paradigm for understanding the first moments of the Universe is known as Inflationary Theory, wherein space rapidly expanded in a very brief period of time [1–4]. An important property of inflation is that its low-energy observables are sensitive to high-energy physics [5, 6]. This non-decoupling of energy scales, while sometimes confounding, can also be used as a probe of ultra high-energy physics such as the effects of quantum gravity. In order to verify, constrain or eliminate classes of such theories, one must understand the precise relationship between low- and high-energy physics in inflationary theory.

The primary low-energy inflationary observables are the correlation functions of primordial perturbations of the quantum field responsible for the inflation. Since such perturbations seed the observed temperature fluctuations in the cosmic microwave background (CMB), one could use the CMB to gain insight into high-energy physics. This is particularly exciting given the recent explosion in precision data by *WMAP* [7], *Planck* [8], *Euclid* [9] and possibly *CMBPol/Inflation Probe* [10].

The inflationary fluctuation spectrum has been observed to be nearly Gaussian [7], and the two-point correlation probes the free theory:

$$\langle \varphi_{\mathbf{k}} \varphi_{\mathbf{p}} \rangle \sim P_{\varphi}(k) (2\pi)^3 \delta^3(\mathbf{k} + \mathbf{p}),$$

Higher-point correlations then probe the interactions by measuring the *non-Gaussianity* of the statistics. The three-point correlation is commonly referred to as the bispectrum and is simply the 3-field analog of the power spectrum:

$$\langle \varphi_{\mathbf{k}_1} \varphi_{\mathbf{k}_2} \varphi_{\mathbf{k}_3} \rangle \sim B_{\varphi}(\mathbf{k}_1, \mathbf{k}_2, \mathbf{k}_3) (2\pi)^3 \delta^3(\mathbf{k}_1 + \mathbf{k}_2 + \mathbf{k}_3). \quad (1)$$

This diagnostic has quickly become an essential tool in constraining inflation models [11]. While as yet there have only been hints of non-Gaussianity [12, 13], a definitive measurement will occur soon from *Planck* [8]. At

the most elementary level, non-Gaussianity can be categorized according to the shape of the triangle formed by the fields’ momentum vectors at which the amplitude B_{φ} is maximized. The ‘squeezed’ shape, $k_1 \sim k_2$ and $k_3 \sim 0$, dominates for local interactions such as $\varphi(x)^3$ [14], and occur well outside the horizon. The ‘equilateral’ shape $k_1 \sim k_2 \sim k_3$ occur primarily at the time of horizon-crossing and dominates for higher-derivative interactions such as found in the Dirac-Born-Infeld theory [15, 16]. The ‘elongated’ shape, where $k_1 + k_2 \sim k_3$, dominates for an initial vacuum state modified away from Bunch-Davies, and often enhances the other types as well [17–22]. A nice heuristic way of understanding this relationship is that the more squeezed the triangle, the later it originated. In anticipation of the upcoming *Planck* data, a more sophisticated technique has recently been pioneered by Fergusson, Liguori, and Shellard [23]. This analysis is model-independent in the sense that it does not assume a particular template shape (squeezed, equilateral, or elongated) and so requires an equally sophisticated model-independent theoretical basis for understanding.

In order to meet this need, the fundamental question how to construct the low-energy effective action in inflationary backgrounds had to be answered. We did so in [24–26]. This new method allows one to reliably compute universal corrections to primordial correlation functions. The approach is model-independent in the sense that we begin with the general form of an ultraviolet-complete action and obtain an answer in terms of a small number of free parameters that in principle encodes all the possible unknown physics. The fundamental organizing principle is not yet known. Nevertheless we can simply compute the effects in any specific model and generalize from there. We have previously used this technique to compute the primordial power spectrum, here we will apply it to compute the 3- and 4-point correlations. An important difference with flat space effective field theory is that a heavy field of mass M will correct the correlation function already at order H/M , where H is the scale of

inflation. Moreover, as will shall show, the leading contribution to the bispectrum is of the elongated shape just as previous studies surmised [17–19, 21, 22].

This article is structured as follows. In §2 we briefly summarize the technical framework by which high-energy physics can consistently be integrated out of a theory in an inflating background. In §3 we calculate the bispectrum corrections, and in §4 those for the trispectrum. In §5 we conclude and offer some remarks about detectability and future directions.

SETUP

The Generic Action

We will consider the most general field theory containing a light scalar field fluctuation φ renormalizably coupled to a heavy field χ :

$$S_{\text{fl}} = \int d^4x \sqrt{g} \left[\frac{1}{2}(\partial\varphi)^2 + \frac{1}{2}(\partial\chi)^2 + \frac{1}{2}M^2\chi^2 + \frac{g_0}{3!}\varphi^3 + \frac{\lambda_0}{4!}\varphi^4 + \frac{g_1}{2}\varphi^2\chi + \frac{\lambda_1}{3!}\varphi^3\chi \right]. \quad (2)$$

This is similar to the theory considered in [24, 25], but we have added a $\varphi^3\chi$ interaction to generate non-Gaussian interactions, and will now include self-interactions in our result [34]. We will take the metric background to be exact de Sitter space,

$$ds^2 = -dt^2 + a(t)^2 dx^2,$$

where $\dot{a}/a \equiv H = \text{constant}$.

The In-In Formalism and Schwinger-Keldysh Basis

In the Schwinger-Keldysh “in-in” formalism, at some early time t_{in} we begin with a pure state $|\text{in}(t_{\text{in}})\rangle$, then evolve the system for the bra- and ket-state separately until some late time t , when we evaluate the expectation value [27]:

$$\begin{aligned} \langle \mathcal{O}(t) \rangle &\equiv \langle \text{in}(t) | \mathcal{O}(t) | \text{in}(t) \rangle \\ &= \langle \text{in}(t_{\text{in}}) | e^{i \int_{t_{\text{in}}}^t dt' H(t')} \mathcal{O}(t) e^{-i \int_{t_{\text{in}}}^t dt'' H(t'')} | \text{in}(t_{\text{in}}) \rangle. \end{aligned} \quad (3)$$

Traditionally, the in-state $|\text{in}\rangle$ is taken to be the Bunch-Davies vacuum state [28], but this is not necessarily so. Expanding cosmological backgrounds allow for a more general class of vacua, which can be heuristically considered to be excited states of inflaton fluctuations. In the present context, we will find that integrating out high-energy physics generically results in corrections to the density matrix, which can be interpreted this way.

If we denote the fields representing the “evolving” ket to be $\{\varphi_+, \chi_+\}$ and those for the “devolving” bra to be

$\{\varphi_-, \chi_-\}$, the in-in expectation value (3) can be computed from the action

$$\mathcal{S} \equiv S[\varphi_+, \chi_+] - S[\varphi_-, \chi_-]. \quad (4)$$

together with the constraint that $\varphi_+(t) = \varphi_-(t)$. It is then helpful to transform into the Keldysh basis,

$$\begin{aligned} \bar{\varphi} &\equiv (\varphi_+ + \varphi_-)/2, & \Phi &\equiv \varphi_+ - \varphi_-, \\ \bar{\chi} &\equiv (\chi_+ + \chi_-)/2, & X &\equiv \chi_+ - \chi_-. \end{aligned}$$

In this basis the action (4) equals

$$\begin{aligned} \mathcal{S}[\bar{\varphi}, \Phi, \bar{\chi}, X] &= - \int d^3\mathbf{x} dt a(t)^3 [\partial\bar{\varphi}\partial\Phi + \partial\bar{\chi}\partial X + M^2\bar{\chi}X \\ &+ \frac{g_0}{2} \left(\bar{\varphi}^2\Phi + \frac{1}{12}\Phi^3 \right) + \frac{\lambda_0}{3!} \left(\bar{\varphi}^3\Phi + \frac{1}{4}\bar{\varphi}\Phi^3 \right) \\ &+ g_1\bar{\varphi}\Phi\bar{\chi} + \frac{g_1}{2}\bar{\varphi}^2X + \frac{\lambda_1}{2}\bar{\varphi}^2\Phi\bar{\chi} + \frac{\lambda_1}{3!}\bar{\varphi}^3X]. \end{aligned}$$

Fluctuation solutions are easiest written in the conformal time τ ,

$$dt \equiv a(\tau)d\tau.$$

The free field solutions are then

$$\begin{aligned} U_{\mathbf{k}}(\tau) &= \frac{H}{\sqrt{2k^3}}(1 - ik\tau)e^{-ik\tau}, \\ V_{\mathbf{k}}(\tau) &\approx \frac{1}{a(\tau)} \frac{\exp\left[-i \int_{\tau_{\text{in}}}^{\tau} dt' \sqrt{k^2 + \frac{M^2}{H^2\tau'^2}}\right]}{\sqrt{2}\left(k^2 + \frac{M^2}{H^2\tau^2}\right)^{1/4}} \end{aligned}$$

where for the latter we have used the WKB approximation which is always valid for $H/M \ll 1$.

We will also need the Green’s and Wightman functions in the Keldysh basis; see [25] for an explanation of their interpretation. Fourier transforming into comoving momentum, the retarded Green’s function G^R can be written in terms of the fluctuation solutions,

$$\begin{aligned} G_{\mathbf{k}}^R(\tau_1, \tau_2) &\equiv i\langle \bar{\varphi}_{\mathbf{k}}(\tau_1)\Phi_{-\mathbf{k}}(\tau_2) \rangle \\ &= -2\theta(\tau_1 - \tau_2)\text{Im}[U_{\mathbf{k}}(\tau_1)U_{\mathbf{k}}^*(\tau_2)]. \end{aligned} \quad (5)$$

The advanced Green’s function G^A is then simply the time-reversal of this:

$$G_{\mathbf{k}}^A(\tau_1, \tau_2) \equiv G_{\mathbf{k}}^R(\tau_2, \tau_1).$$

A similar procedure applies for $\bar{\chi}$ using its corresponding retarded Green’s function \mathcal{G}^R ,

$$\begin{aligned} \mathcal{G}_{\mathbf{k}}^R(\tau_1, \tau_2) &\equiv i\langle \bar{\chi}_{\mathbf{k}}(\tau_1)X_{-\mathbf{k}}(\tau_2) \rangle \\ &= -2\theta(\tau_1 - \tau_2)\text{Im}[V_{\mathbf{k}}(\tau_1)V_{\mathbf{k}}^*(\tau_2)]. \end{aligned} \quad (6)$$

The Wightman functions are

$$\begin{aligned} F_{\mathbf{k}}(\tau_1, \tau_2) &= \langle \bar{\varphi}_{\mathbf{k}}(\tau_1)\bar{\varphi}_{-\mathbf{k}}(\tau_2) \rangle \\ &= \text{Re}[U_{\mathbf{k}}(\tau_1)U_{\mathbf{k}}^*(\tau_2)], \\ 0 &= \langle \Phi_{\mathbf{k}}(\tau_1)\Phi_{-\mathbf{k}}(\tau_2) \rangle, \\ \mathcal{F}_{\mathbf{k}}(\tau_1, \tau_2) &= \langle \bar{\chi}_{\mathbf{k}}(\tau_1)\bar{\chi}_{-\mathbf{k}}(\tau_2) \rangle \\ &= \text{Re}[V_{\mathbf{k}}(\tau_1)V_{\mathbf{k}}^*(\tau_2)], \\ 0 &= \langle X_{\mathbf{k}}(\tau_1)X_{-\mathbf{k}}(\tau_2) \rangle. \end{aligned}$$

We will now use these to compute higher-point correlation functions in the interacting theory.

BISPECTRUM CORRECTIONS

Definitions

A more precise definition of the bispectrum given by eq. (1) is

$$B_\varphi(\mathbf{k}_1, \mathbf{k}_2, \mathbf{k}_3)(2\pi)^3 \delta^3(\mathbf{k}_1 + \mathbf{k}_2 + \mathbf{k}_3) \equiv \langle \text{in}(0) | \bar{\varphi}_{\mathbf{k}_1}(0) \bar{\varphi}_{\mathbf{k}_2}(0) \bar{\varphi}_{\mathbf{k}_3}(0) | \text{in}(0) \rangle, \quad (7)$$

where the time evolution of the in-state is given by

$$|\text{in}(\tau)\rangle = e^{-i \int_{\tau_{\text{in}}}^{\tau} dt' \mathcal{H}(t')} |\text{in}(\tau_{\text{in}})\rangle,$$

recalling that $\tau \rightarrow 0^-$ corresponds to future infinity. From henceforth we will assume a Bunch-Davies in-state. There are two types of contributions to B_φ : those arising from self-interactions of the φ field, and those mediated by the heavy field χ coupled to φ . Since they have qualitatively different behavior, we will consider each separately.

Self Interactions

Let us first consider the simplest possible interaction: that arising from the φ^3 interaction. In the Schwinger-Keldysh basis this produces two diagrams, shown in Figure 1. These are given by (we henceforth omit the momentum-conserving delta-function and just assume that $\mathbf{k}_1 + \mathbf{k}_2 + \mathbf{k}_3 = 0$):

$$B_\varphi^{\text{self}} = \frac{(-ig_0)}{(2\pi)^3} \int_{\tau_{\text{in}}}^0 d\tau a(\tau)^4 \times \left([-iG_{\mathbf{k}_1}^R(0, \tau)] F_{\mathbf{k}_2}(0, \tau) F_{\mathbf{k}_3}(0, \tau) + \text{permutations} + \frac{1}{4} [-iG_{\mathbf{k}_1}^R(0, \tau)] [-iG_{\mathbf{k}_2}^R(0, \tau)] [-iG_{\mathbf{k}_3}^R(0, \tau)] \right).$$

Writing out the Green and Wightman functions in terms of the functions $U_{\mathbf{k}}(\tau)$, $U_{\mathbf{k}}^*(\tau)$, and using the fact that $U_{\mathbf{k}}(0) = U_{\mathbf{k}}^*(0) = H/\sqrt{2k^3}$ yields

$$B_\varphi^{\text{self}} = \frac{ig_0}{2(2\pi)^3 (2k_1 k_2 k_3)^{3/2} H} \int_{\tau_{\text{in}}}^0 \frac{d\tau}{\tau^4} \left[U_{\mathbf{k}_1}(\tau) U_{\mathbf{k}_2}(\tau) U_{\mathbf{k}_3}(\tau) + U_{\mathbf{k}_1}^*(\tau) U_{\mathbf{k}_2}(\tau) U_{\mathbf{k}_3}(\tau) + \text{permutations} - \text{c.c.} \right].$$

The integrals will converge in the far past by slightly rotating the path of integration into the complex plane, so that $\tau_{\text{in}} \rightarrow -\infty(1+i\epsilon)$. For the far future, we choose



FIG. 1: Lowest-order contributions to primordial bispectrum induced by the self-interaction of the light field. Single solid lines indicate contractions of $\bar{\varphi}$, dashed single lines indicate those of Φ .

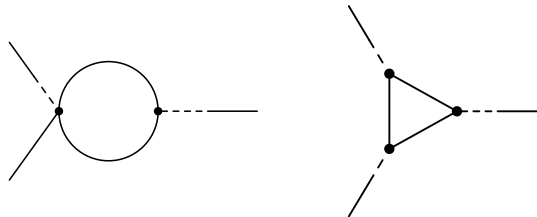


FIG. 2: Higher-order bispectrum contribution induced by multiple self-interactions of the light field. These can be neglected in slow-roll inflation due to the strong constraints on the couplings.

a cutoff at $\mu \rightarrow 0^-$, so that the most singular part of the resultant integrals are:

$$\int_{-\infty(1+i\epsilon)}^{\mu} \frac{d\tau}{\tau^n} e^{-ik\tau} \sim -\frac{\mu^{1-n}}{n-1} + \mathcal{O}((k\mu)^{-n}). \quad (8)$$

Thus the late-time correlation is approximately

$$B_\varphi^{\text{self}} \approx \frac{g_0 \mu^{-3} H^2}{6(2\pi k_1 k_2 k_3)^3}.$$

This correlation peaks when $k_i \approx 0$, corresponding to the squeezed shapes of the momentum triangle. Note that this is *not* quite the same local interaction studied by Komatsu and Spergel [14], which introduce nonlinearities into the late-time gauge-independent parameter ζ , whereas we deal with the field fluctuation φ and integrate the interactions from the far past. Defining the non-linearity parameter $f_{\text{NL}}^{\text{self}} \sim B_\varphi^{\text{self}}/P_\varphi^2 \sim k^{-3}$, the self interaction is seen to have a strong red scaling. This may possibly be measurable in the near future [31] using the leverage provided by combining the *Planck* [8] and *Euclid* [9] datasets. Employing two self interactions will produce loop corrections of order $B_\varphi^{\text{self}} \sim g_0 \lambda_0 H^2$ and $B_\varphi^{\text{self}} \sim g_0^3$ as shown in Figure 2, but slow-roll assumes that these couplings are small and so these contributions are subleading.

High-Energy Correction A

We now turn to the corrections generated by high-energy physics. To leading order in the heavy field, there

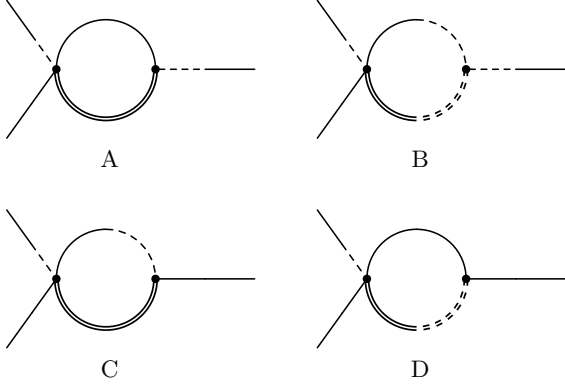


FIG. 3: Contributions to primordial non-Gaussianity induced by the heavy field. The double lines indicate the heavy field components $\{\bar{\chi}, X\}$, with notation analogous to Figure 1.

are four such corrections, shown diagrammatically in Figure 3. Since $\tau_2 \leq \tau_1$ we need only consider corrections containing $G^R(\tau_1, \tau_2)$ (as opposed to corrections containing $G^A(\tau_1, \tau_2)$).

The first correction is given by

$$B_\varphi^A = \frac{(-ig_1)(-i\lambda_1)}{(2\pi)^3} \int_{\tau_{\text{in}}}^0 d\tau_1 a(\tau_1)^4 \int_{\tau_{\text{in}}}^0 d\tau_2 a(\tau_2)^4 \times \int \frac{d^3\mathbf{q}}{(2\pi)^3} \left([-iG_{\mathbf{k}_1}^R(0, \tau_1)] F_{\mathbf{k}_2}(0, \tau_1) F_{\mathbf{q}}(\tau_1, \tau_2) \times \mathcal{F}_{\mathbf{q}-\mathbf{k}_3}(\tau_1, \tau_2) [-iG_{\mathbf{k}_3}^A(\tau_2, 0)] + \text{permutations} \right).$$

Writing out the Green and Wightman functions in terms of U 's and V 's, we see there are now several types of vertices, depending on the permutation of conjugation. The first is

$$\begin{aligned} \mathcal{A}_1(\mathbf{k}_1, \mathbf{k}_2) &\equiv \int_{\tau_{\text{in}}}^0 d\tau a(\tau)^4 U_{\mathbf{k}_1}(\tau) U_{\mathbf{k}_2}(\tau) V_{-(\mathbf{k}_1+\mathbf{k}_2)}^*(\tau) f(\tau) \\ &= -\frac{1}{2\sqrt{2k_1^3 k_2^3} H} \int_{\tau_{\text{in}}}^0 \frac{d\tau}{\tau^3} \frac{(1-ik_1\tau)(1-ik_2\tau)}{(|\mathbf{k}_1+\mathbf{k}_2|^2 + \frac{M^2}{H^2\tau^2})^{1/4}} f(\tau) \\ &\times \exp \left[-i(k_1+k_2)\tau + i \int_{\tau_{\text{in}}}^{\tau} d\tau' \sqrt{|\mathbf{k}_1+\mathbf{k}_2|^2 + \frac{M^2}{H^2\tau'^2}} \right], \end{aligned}$$

where we have introduced a function $f(\tau)$ to account for any step-functions. As first noted in [24], by rescaling $u \equiv H\tau/M$ the vertex $\mathcal{A}_1(\mathbf{k}_1, \mathbf{k}_2)$ admits a stationary phase approximation at the energy-conservation moment

$$k_1 + k_2 = \sqrt{|\mathbf{k}_1 + \mathbf{k}_2|^2 + u_c^{-2}}. \quad (9)$$

The solution to this defines the New Physics Hypersurface (NPH),

$$u_c^{-1} = -\sqrt{2k_1 k_2 (1 - \cos \theta)}, \quad \cos \theta = \frac{\mathbf{k}_1 \cdot \mathbf{k}_2}{k_1 k_2}.$$

Then to leading order in H/M the amplitude is

$$\begin{aligned} \mathcal{A}_1(\mathbf{k}_1, \mathbf{k}_2) &\approx -\frac{\sqrt{\pi} i f(\tau_c) e^{-i\frac{M}{H} \sqrt{|\mathbf{k}_1+\mathbf{k}_2|^2 u_{\text{in}}^2 + 1}}}{2\sqrt{k_1 k_2} [2k_1 k_2 (1 - \cos \theta)]^{1/4} \sqrt{HM}} \\ &\times \left(\frac{k_1 + k_2 + \sqrt{2k_1 k_2 (1 - \cos \theta)}}{\sqrt{|\mathbf{k}_1 + \mathbf{k}_2|^2 + u_{\text{in}}^{-2} + |u_{\text{in}}|^{-1}}} \right)^{-i\frac{M}{H}}. \quad (10) \end{aligned}$$

The physics of this is clear. This diagram accounts for the threshold production/decay of heavy particles at high redshift in the early universe. Note that in order to evaluate $f(\tau_c)$, one should use the step-function appropriately ‘‘averaged’’ due to the Gaussian fluctuations:

$$\theta(\tau) = \begin{cases} 1 & \text{if } \tau > 0, \\ 1/2 & \text{if } \tau = 0, \\ 0 & \text{if } \tau < 0. \end{cases} \quad (11)$$

The second possible vertex is identical to \mathcal{A}_1 but with one U conjugated. This has only imaginary-time saddle-point solutions. Since our τ -integral is confined to the real axis we will never pass over this point in our integration, and so this amplitude will be suppressed as $\mathcal{A}_2 \sim \text{erf}(\frac{M}{H}) \sim \frac{H}{M} e^{-(M/H)^2}$, allowing us to neglect such interactions. Finally we consider \mathcal{A}_3 which has both U 's conjugated and so admits no saddlepoint solutions, and thus can also be neglected. Note also that while there are actually two solutions (differing in sign), we limit ourselves to the solution for which $u_c < 0$, corresponding to the inflating phase (see [25] for details on this).

We can now perform a similar analysis of four-field interactions. The first such vertex is

$$\begin{aligned} \mathcal{B}_1(\mathbf{k}_1, \mathbf{k}_2, \mathbf{k}_3) &\equiv \int_{\tau_{\text{in}}}^0 d\tau a(\tau)^4 U_{\mathbf{k}_1}(\tau) U_{\mathbf{k}_2}(\tau) U_{\mathbf{k}_3}(\tau) V_{-(\mathbf{k}_1+\mathbf{k}_2+\mathbf{k}_3)}^*(\tau) f(\tau) \\ &= -\frac{1}{4\sqrt{k_1^3 k_2^3 k_3^3} H} \int_{\tau_{\text{in}}}^0 \frac{d\tau}{\tau^3} \frac{(1-ik_1\tau)(1-ik_2\tau)(1-ik_3\tau)}{(|\mathbf{k}_1+\mathbf{k}_2+\mathbf{k}_3|^2 + \frac{M^2}{H^2\tau^2})^{1/4}} \\ &\times \exp \left[-i(k_1+k_2+k_3)\tau + i \int_{\tau_{\text{in}}}^{\tau} d\tau' \sqrt{|\mathbf{k}_1+\mathbf{k}_2+\mathbf{k}_3|^2 + \frac{M^2}{H^2\tau'^2}} \right]. \end{aligned}$$

Using the same rescaling, the stationary phase is now at

$$u_c^{-1} = -\sqrt{(k_1+k_2+k_3)^2 - |\mathbf{k}_1+\mathbf{k}_2+\mathbf{k}_3|^2}$$

which always exists (that is, it is real). To leading order, the amplitude is

$$\begin{aligned} \mathcal{B}_1(\mathbf{k}_1, \mathbf{k}_2, \mathbf{k}_3) &\approx \frac{i\sqrt{\pi} i M f(\tau_c) e^{-i\frac{M}{H} \sqrt{|\mathbf{k}_1+\mathbf{k}_2+\mathbf{k}_3|^2 u_{\text{in}}^2 + 1}}}{4\sqrt{H k_1 k_2 k_3}} \\ &\times [(k_1+k_2+k_3)^2 - |\mathbf{k}_1+\mathbf{k}_2+\mathbf{k}_3|^2]^{-3/4} \\ &\times \left(\frac{k_1+k_2+k_3 + \sqrt{(k_1+k_2+k_3)^2 - |\mathbf{k}_1+\mathbf{k}_2+\mathbf{k}_3|^2}}{\sqrt{|\mathbf{k}_1+\mathbf{k}_2+\mathbf{k}_3|^2 + u_{\text{in}}^{-2} + |u_{\text{in}}|^{-1}}} \right)^{-i\frac{M}{H}}. \end{aligned}$$

A similar vertex, but with the third light field outgoing (we place a bar there to remind us of this), is:

$$\begin{aligned} \mathcal{B}_2(\mathbf{k}_1, \mathbf{k}_2 | \mathbf{k}_3) &\equiv \int_{\tau_{\text{in}}}^0 d\tau a(\tau)^4 U_{\mathbf{k}_1}(\tau) U_{\mathbf{k}_2}(\tau) U_{\mathbf{k}_3}^*(\tau) V_{-(\mathbf{k}_1 + \mathbf{k}_2 + \mathbf{k}_3)}^*(\tau) f(\tau) \\ &= -\frac{1}{4\sqrt{k_1^3 k_2^3 k_3^3}} \int_{\tau_{\text{in}}}^0 \frac{d\tau}{\tau^3} \frac{(1 - ik_1\tau)(1 - ik_2\tau)(1 + ik_3\tau)}{(|\mathbf{k}_1 + \mathbf{k}_2 + \mathbf{k}_3|^2 + \frac{M^2}{H^2\tau^2})^{1/4}} \\ &\times \exp \left[-i(k_1 + k_2 - k_3)\tau + i \int_{\tau_{\text{in}}}^{\tau} d\tau' \sqrt{|\mathbf{k}_1 + \mathbf{k}_2 + \mathbf{k}_3|^2 + \frac{M^2}{H^2\tau'^2}} \right]. \end{aligned}$$

The stationary phase for this is at

$$u_c^{-1} = -\sqrt{(k_1 + k_2 - k_3)^2 - |\mathbf{k}_1 + \mathbf{k}_2 + \mathbf{k}_3|^2}.$$

This is *not* always real, and one must take care. To leading order, the amplitude is

$$\begin{aligned} \mathcal{B}_2(\mathbf{k}_1, \mathbf{k}_2 | \mathbf{k}_3) &\approx \frac{i\sqrt{\pi i M} f(\tau_c) e^{-i\frac{M}{H}\sqrt{|\mathbf{k}_1 + \mathbf{k}_2 + \mathbf{k}_3|^2 u_{\text{in}}^2 + 1}}}{4\sqrt{H k_1 k_2 k_3}} \\ &\times [(k_1 + k_2 - k_3)^2 - |\mathbf{k}_1 + \mathbf{k}_2 + \mathbf{k}_3|^2]^{-3/4} \\ &\times \left(\frac{k_1 + k_2 - k_3 + \sqrt{(k_1 + k_2 - k_3)^2 - |\mathbf{k}_1 + \mathbf{k}_2 + \mathbf{k}_3|^2}}{\sqrt{|\mathbf{k}_1 + \mathbf{k}_2 + \mathbf{k}_3|^2 + u_{\text{in}}^{-2} + |u_{\text{in}}|^{-1}}} \right)^{-i\frac{M}{H}} \end{aligned}$$

Based on this, it is easy to see that the amplitude is

$$\begin{aligned} B_\varphi^A &= \frac{g_1 \lambda_1}{8(2\pi)^3} \frac{H^3}{(2k_1 k_2 k_3)^{3/2}} \int \frac{d^3 \mathbf{q}}{(2\pi)^3} \\ &\left[\mathcal{A}_1(\mathbf{q}, -\mathbf{k}_3) \mathcal{B}_1^*(\mathbf{k}_2, \mathbf{q}, \mathbf{k}_1) + \text{c.c.} \right. \\ &\left. - \mathcal{A}_1(\mathbf{q}, -\mathbf{k}_3) \mathcal{B}_2^*(\mathbf{k}_2, \mathbf{q} | \mathbf{k}_1) + \mathcal{A}_1(\mathbf{q}, -\mathbf{k}_3) \mathcal{B}_2^*(\mathbf{k}_1, \mathbf{q} | \mathbf{k}_2) + \text{c.c.} \right. \\ &\left. + \text{permutations} \right]. \end{aligned}$$

But the $k_1 \leftrightarrow k_2$ symmetry will cancel the \mathcal{B}_2 -dependent terms, leaving only the \mathcal{B}_1 -dependent terms.

Examining the loop integral in the expression above, the integrand contains a rapidly oscillating component due to the difference in vertex interaction times is

$$\left(\frac{|\mathbf{k}_1 + \mathbf{k}_2| + q + \sqrt{(|\mathbf{k}_1 + \mathbf{k}_2| + q)^2 - |\mathbf{k}_1 + \mathbf{k}_2 + \mathbf{q}|^2}}{k_1 + k_2 + q + \sqrt{(k_1 + k_2 + q)^2 - |\mathbf{k}_1 + \mathbf{k}_2 + \mathbf{q}|^2}} \right)^{-i\frac{M}{H}}. \quad (12)$$

Given such rapid oscillations of this phase, this could potentially be evaluated using (another) stationary phase approximation. However, one can easily convince themselves that there exist no such stationary phase points except in the trivial case of $k_3 = |\mathbf{k}_1 + \mathbf{k}_2| = k_1 + k_2$, meaning the phase is identically zero. Thus, for all configurations except this, the amplitude is suppressed as H/M .

To evaluate the integral, we then expand near this point,

$$\kappa_{12} \equiv k_1 + k_2 - k_3,$$

and the oscillating component (12) simplifies to

$$e^{i\frac{M}{H}\kappa_{12}/\sqrt{2qk_3(1-\cos\theta)}},$$

where θ is the angle between $-\mathbf{k}_3 = \mathbf{k}_1 + \mathbf{k}_2$ and \mathbf{q} .

Now we must do the integral over \mathbf{q} . As done in earlier work [24, 25], we first use the azimuthal symmetry around \mathbf{k}_3 to simplify the 3d integral into just two variables,

$$\int \frac{d^3 \mathbf{q}}{(2\pi)^3} \rightarrow \frac{1}{(2\pi)^2} \int q^2 dq d(1 - \cos\theta).$$

We wish to transform this into the (u, E) -basis given by

$$u^{-1} \equiv -\sqrt{2k_3 q(1 - \cos\theta)}, \quad (13)$$

$$E \equiv Mq|u| = M\sqrt{\frac{q}{2k_3(1 - \cos\theta)}}.$$

These can be easily inverted as

$$q = \frac{E}{M|u|}, \quad 1 - \cos\theta = \frac{M}{2k_3 E|u|},$$

so that the \mathbf{q} -integral then transforms as

$$\int \frac{d^3 \mathbf{q}}{(2\pi)^3} \rightarrow -\frac{1}{(2\pi)^2 M^2 k_3} \int \frac{du E dE}{u^5}. \quad (14)$$

The integrand transforms as

$$\mathcal{A}_1(\mathbf{q}, -\mathbf{k}_3) \mathcal{B}_1^*(\mathbf{k}_2, \mathbf{q}, \mathbf{k}_1) \rightarrow \frac{\pi|u|^3 M e^{-i\frac{M}{H}\kappa_{12}u}}{8HE\sqrt{k_1 k_2 k_3}} + \mathcal{O}(\kappa_{12}). \quad (15)$$

Noting that E is a physical rather than a comoving scale, we can now easily place limits on the region of integration in terms of the physical cutoff Λ . Recalling that at the moment of interaction the energies of the light fields will sum to the energy of the heavy field, and so it is this latter quantity that we must place the bound of Λ on. The minimal energy bound comes from the geometrical constraint $\cos\theta \geq -1$. The bounds on the loop energy are then:

$$\begin{aligned} \frac{M}{4k_3|u|} &\leq E \leq \Lambda - k_3|u|M, \\ -\frac{\Lambda + \sqrt{\Lambda^2 - M^2}}{2Mk_3} &\leq u \leq -\frac{\Lambda - \sqrt{\Lambda^2 - M^2}}{2Mk_3}. \end{aligned}$$

The measure (14) and integrand (15) combine to produce an E -integral which is trivial,

$$\int_{\frac{M}{4k_3|u|}}^{\Lambda - k_3|u|M} dE = \Lambda - k_3|u|M - \frac{M}{4k_3|u|}.$$

Now including the factor of u^{-2} from the measure and vertex evaluations (15) we can well-approximate the remaining integral over u as Gaussian near the peak at

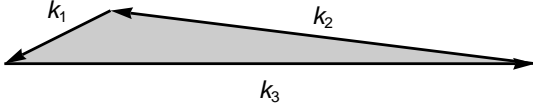


FIG. 4: Example of an ‘elongated’ bispectrum momentum-vector triangle which can be produced from high-energy physics, where $k_1 + k_2 \approx k_3$.

$$u_0 \approx -3M/8\Lambda k_3,$$

$$\begin{aligned} & |u|^{-2} \left[\Lambda - k_3 |u| M - \frac{M}{4k_3 |u|} \right] \\ & \approx \frac{\Lambda}{3} \left(\frac{8\Lambda k_3}{3M} \right)^2 \exp \left[-\frac{27}{6} \left(\frac{\Lambda k_3}{M} \right)^2 (u - u_0)^2 \right] + \mathcal{O} \left(\frac{M}{\Lambda} \right). \end{aligned}$$

Extending the domain of integration to $u \in (-\infty, \infty)$, the integral over u can then be easily performed to yield another Gaussian for κ_{12} . The exponential will cut off anything beyond $\kappa_{12} \approx 2^4 k_3 \Lambda H / \sqrt{3} M^2$, by which time the phase will have completed about half a cycle. Thus we can approximate this as a delta-function,

$$\begin{aligned} & \int_{-\infty}^{\infty} du e^{-i\frac{M}{H}\kappa_{12}u - \frac{27}{6} \left(\frac{\Lambda k_3}{M} \right)^2 (u - u_0)^2} + \text{c.c.} \\ & \approx \sqrt{\frac{6\pi}{25}} \left(\frac{M}{\Lambda k_3} \right) e^{-i\frac{M}{H}\kappa_{12}u_0 - \frac{3}{25} \left(\frac{M^2 \kappa_{12}}{H\Lambda k_3} \right)^2} + \text{c.c.} \\ & \approx \frac{4\pi H}{M} \delta(\kappa_{12}). \end{aligned}$$

An important caveat is that corrections to this approximation will be of order $\Lambda H/M^2$, necessitating that this be a small quantity. This is the same restriction one obtains for using the plane wave approximation $U_{\mathbf{k}} \approx \frac{H\tau}{\sqrt{2k}} e^{-ik\tau}$ for all interactions and so is already implicitly assumed. The final answer is then

$$B_{\varphi}^A \approx \frac{\pi g_1 \lambda_1 H^3 \Lambda^3}{27\sqrt{2}(2\pi)^4 M^4 k_1^2 k_2^2 k_3} \delta(k_1 + k_2 - k_3) + \text{perms.} \quad (16)$$

The requirement that $k_1 + k_2 \approx k_3$ implies that the momentum-vector diagram approximates an elongated triangle, as shown in Figure 4. The fact that modifications to the initial state produce the elongated type of non-Gaussianity was anticipated by [17–19]; here we see how this originates from fundamental high-energy physics. The factor of $(\Lambda/M)^3$ can be absorbed into the bare couplings g_1, λ_1 . Since $g_1 \sim H, \lambda_1 \sim 1, \Lambda/M \sim 1$, the correction (16) will then scale as $B_{\varphi}^A \sim H/M$. The nonlinearity parameter scaling as $f_{\text{NL}}^A \sim B_{\varphi}^A/P_{\varphi}^2$ is scale-invariant, so $n_{\text{NL}}^A \equiv d \ln f_{\text{NL}}^A / d \ln k = 0$.

High-Energy Correction B

The next diagram is very similar,

$$\begin{aligned} B_{\varphi}^B &= \frac{(-ig_1)(-i\lambda_1)}{(2\pi)^3} \int_{\tau_{\text{in}}}^0 d\tau_1 a(\tau_1)^4 \int_{\tau_{\text{in}}}^0 d\tau_2 a(\tau_2)^4 \times \\ & \int \frac{d^3\mathbf{q}}{(2\pi)^3} \left([-iG_{\mathbf{k}_1}^R(0, \tau_1)] F_{\mathbf{k}_2}(0, \tau_1) [-iG_{\mathbf{q}}^R(\tau_1, \tau_2)] \times \right. \\ & \left. [-i\mathcal{G}_{\mathbf{q}-\mathbf{k}_3}^R(\tau_1, \tau_2)] [-iG_{\mathbf{k}_3}^A(\tau_2, 0)] + \text{permutations} \right). \end{aligned}$$

We do not need to explicitly evaluate this, however, because in the stationary phase approximation this is easily seen to be identical to diagram A but with a minus sign and the Heaviside function $\theta(\tau_1 - \tau_2)$. This allows us to integrate over only half the fluctuations in τ_1, τ_2 and hence we get

$$B_{\varphi}^B = -\frac{1}{2} B_{\varphi}^A.$$

High-Energy Corrections C and D

There are two additional diagrams from high-energy interactions,

$$\begin{aligned} B_{\varphi}^C &= \frac{(-ig_1)(-i\lambda_1)}{(2\pi)^3} \int_{\tau_{\text{in}}}^0 d\tau_1 a(\tau_1)^4 \int_{\tau_{\text{in}}}^0 d\tau_2 a(\tau_2)^4 \times \\ & \int \frac{d^3\mathbf{q}}{(2\pi)^3} \left([-iG_{\mathbf{k}_1}^R(0, \tau_1)] F_{\mathbf{k}_2}(0, \tau_1) [-iG_{\mathbf{q}}^R(\tau_1, \tau_2)] \times \right. \\ & \left. \mathcal{F}_{\mathbf{q}-\mathbf{k}_3}(\tau_1, \tau_2) F_{\mathbf{k}_3}(\tau_2, 0) + \text{permutations} \right), \\ B_{\varphi}^D &= \frac{(-ig_1)(-i\lambda_1)}{(2\pi)^3} \int_{\tau_{\text{in}}}^0 d\tau_1 a(\tau_1)^4 \int_{\tau_{\text{in}}}^0 d\tau_2 a(\tau_2)^4 \times \\ & \int \frac{d^3\mathbf{q}}{(2\pi)^3} \left([-iG_{\mathbf{k}_1}^R(0, \tau_1)] F_{\mathbf{k}_2}(0, \tau_1) F_{\mathbf{q}}(\tau_1, \tau_2) \times \right. \\ & \left. [-i\mathcal{G}_{\mathbf{q}-\mathbf{k}_3}^R(\tau_1, \tau_2)] F_{\mathbf{k}_3}(\tau_2, 0) + \text{permutations} \right). \end{aligned}$$

This time, the stationary phase approximation implies the total cancellation of these terms against each other. As first observed in the power spectrum calculation [24], this is a general theme: the leading-order corrections arising from the dynamics effective action will cancel, and the dominant corrections by power counting arise entirely from the density matrix.

Total Bispectrum

The complete bispectrum correction is then

$$B_{\varphi} = B_{\varphi}^{\text{self}} + B_{\varphi}^A + B_{\varphi}^B.$$

The high-energy physics produces a scale-invariant elongated shape of bispectrum corrections.

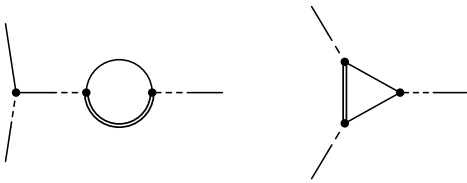


FIG. 5: Examples of 3-point diagrams which are model-dependent, and so not considered here.

There are a few other diagrams involving high-energy interactions shown in Figure 5, but they all involve a local or derivative coupling (strongly constrained by slow-roll), as well as a factor of H/M . Thus, these model-dependent terms will be subleading to the diagrams computed here. In non-slow roll models local terms may significantly contribute and in fact correspond precisely to the terms discussed in [19]. The vacuum modification should also enhance local interactions, as first found in [21, 22]. Higher-derivative actions (for example, DBI [16] or more generally [30]) favor large equilateral bispectra [15], although will likely contain new features due to the high-energy physics.

TRISPECTRUM CORRECTIONS

The 4-point correlation, or trispectrum, is defined analogously to the bispectrum:

$$T_\varphi(\mathbf{k}_1, \mathbf{k}_2, \mathbf{k}_3, \mathbf{k}_4)(2\pi)^3 \delta^3(\mathbf{k}_1 + \mathbf{k}_2 + \mathbf{k}_3 + \mathbf{k}_4) \equiv \langle \text{in}(0) | \varphi_{\mathbf{k}_1}(0) \varphi_{\mathbf{k}_2}(0) \varphi_{\mathbf{k}_3}(0) \varphi_{\mathbf{k}_4}(0) | \text{in}(0) \rangle. \quad (17)$$

It was suggested in [25] that highly oscillatory corrections to power spectrum may be invisible, yet show up in the trispectrum as enhanced variance. This is because the dominant contribution to the trispectrum is the power spectrum-squared,

$$T_\varphi \sim \delta^3(\mathbf{k}_1 - \mathbf{k}_2) \delta^3(\mathbf{k}_3 - \mathbf{k}_4) P_\varphi(k_1) P_\varphi(k_3) + \text{permutations}.$$

A modification in P_φ of order H/M would then produce a change of order $2P_\varphi H/M$ in T_φ . Below we will evaluate the corrections to T_φ , due to self- and high-energy interactions. We will see that this is not true.

Self Interactions

The first non-factorizable contribution will be from the self-interaction as shown in Figure 6, again using a late-time cutoff $\mu \rightarrow 0^-$ and the most singular part of the

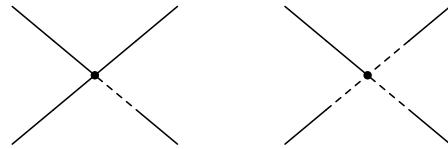


FIG. 6: Contributions to the trispectrum from self-interactions. There are also $\mathcal{O}(g_0^2)$ and $\mathcal{O}(\lambda_0^2)$ contributions which we can neglect in slow-roll inflation due to the strong constraints on the couplings.

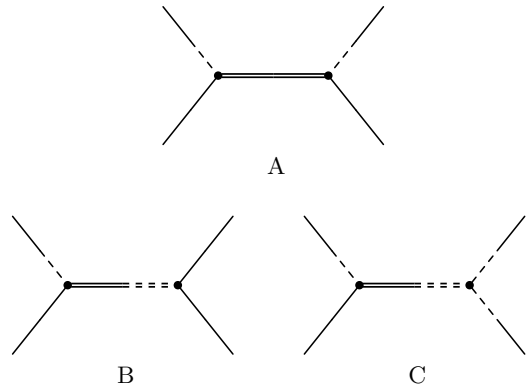


FIG. 7: Tree-level high-energy contributions to the 4-point correlation function.

exponential integral given by (8),

$$\begin{aligned} T_\varphi^{\text{self}} &= \frac{(-i\lambda_0)}{(2\pi)^3} \int_{-\infty(1+i\epsilon)}^\mu d\tau a(\tau)^4 \times \\ &\left(F_{\mathbf{k}_1}(0, \tau) F_{\mathbf{k}_2}(0, \tau) F_{\mathbf{k}_3}(0, \tau) [-iG_{\mathbf{k}_4}^R(0, \tau)] + \text{permutations} \right. \\ &\left. + F_{\mathbf{k}_1}(0, \tau) [-iG_{\mathbf{k}_2}^R(0, \tau)] [-iG_{\mathbf{k}_3}^R(0, \tau)] [-iG_{\mathbf{k}_4}^R(0, \tau)] \right. \\ &\left. + \text{permutations} \right) \\ &= \frac{i\lambda_0}{8(2\pi)^3 (k_1 k_2 k_3 k_4)^{3/2}} \int_{-\infty(1+i\epsilon)}^\mu \frac{d\tau}{\tau^4} \times \\ &\left[U_{\mathbf{k}_1}^*(\tau) U_{\mathbf{k}_2}(\tau) U_{\mathbf{k}_3}(\tau) U_{\mathbf{k}_4}(\tau) + \text{permutations} - \text{c.c.} \right] \\ &\approx \frac{\lambda_0 \mu^{-3} H^4}{24(2\pi k_1 k_2 k_3 k_4)^3}. \end{aligned}$$

Such local trispectrum correlation functions clearly peaks at $k_i \approx 0$, and has been studied in [32]. This has a non-linearity parameter $g_{\text{NL}}^{\text{self}} \sim T_\varphi^{\text{self}} / P_\varphi^3 \sim k^{-3}$ scaling. There will also be corrections of order $T_\varphi \sim g_0^2 H^2$ and $T_\varphi \sim \lambda_0^2 H^4$, which are again presumed negligible from slow-roll constraints.

Tree-Level High-Energy Corrections

Figure 7 shows the three tree-level high-energy diagrams contributing to the trispectrum corrections. We

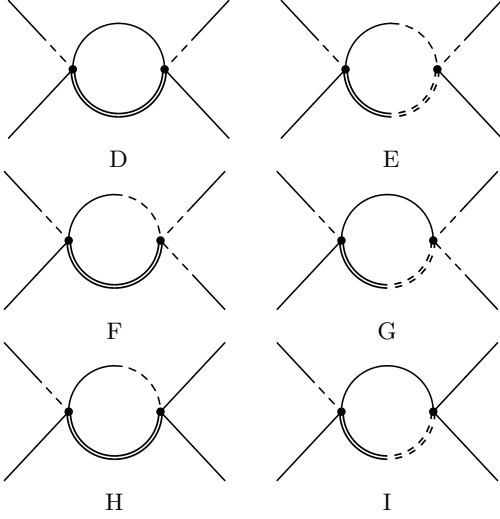


FIG. 8: Loop high-energy contributions to the 4-point correlation function.

first evaluate diagram A,

$$\begin{aligned}
T_\varphi^A &= \frac{(-ig_1)^2}{(2\pi)^3} \int_{\tau_{\text{in}}}^0 d\tau_1 a(\tau_1)^4 \int_{\tau_{\text{in}}}^0 d\tau_2 a(\tau_2)^4 \times \\
&\quad \left([-iG_{\mathbf{k}_1}^R(0, \tau_1)] F_{\mathbf{k}_2}(0, \tau_1) \mathcal{F}_{\mathbf{k}_1+\mathbf{k}_2}(\tau_1, \tau_2) \times \right. \\
&\quad \left. [-iG_{\mathbf{k}_3}^A(\tau_2, 0)] F_{\mathbf{k}_4}(\tau_2, 0) + \text{permutations} \right) \\
&= \frac{g_1^2 H^4}{4(16\pi^2 k_1 k_2 k_3 k_4)^{3/2}} \left[\mathcal{A}_1(\mathbf{k}_1, \mathbf{k}_2) \mathcal{A}_1^*(\mathbf{k}_3, \mathbf{k}_4) + \text{c.c.} \right] \\
&= \frac{g_1^2 H^3}{2^{10} \pi^2 (k_1 k_2 k_3 k_4)^2 M} \times \\
&\quad [(k_1 + k_2)^2 - |\mathbf{k}_1 + \mathbf{k}_2|^2]^{-1/4} [(k_3 + k_4)^2 - |\mathbf{k}_3 + \mathbf{k}_4|^2]^{-1/4} \times \\
&\quad \left(\frac{k_1 + k_2 + \sqrt{(k_1 + k_2)^2 - |\mathbf{k}_1 + \mathbf{k}_2|^2}}{k_3 + k_4 + \sqrt{(k_3 + k_4)^2 - |\mathbf{k}_3 + \mathbf{k}_4|^2}} \right)^{-iM/H} + \text{c.c.} \\
&\quad + \text{permutations.}
\end{aligned}$$

As in the bispectrum, the oscillating phase corresponds to the difference in interaction time between the two vertices. In this case, however, there is no loop-momentum integration to wash the oscillations out. That these oscillations are really present is in fact easy to understand. Due to the cosmological blueshift the difference in interaction times translates into a difference in energies. The Schwinger-Keldysh-Feynman diagram describes a coherent pair of heavy particles spontaneously created each separately decaying into light particles at different moments where the on-shell condition is reached. One can therefore effectively think of the heavy particle as a superposition of “two” states, $|\chi\rangle = \frac{1}{\sqrt{1+|\alpha|^2}} (|\chi_1\rangle + \alpha|\chi_2\rangle)$, one state χ_1 which decays to $\chi_1 \rightarrow \varphi(k_1) + \varphi(k_2)$, the other to $\chi_2 \rightarrow \varphi(k_3) + \varphi(k_4)$. Moreover (though energy is not a good quantum number

in cosmology) the effective energy encoded in the interaction time is different for χ_1 and χ_2 . A state which is a superposition of two different energy states with respective energies E_1, E_2 and lifetimes τ_1, τ_2 famously shows oscillations in its time evolution:

$$\begin{aligned}
|\langle \chi(t) | \chi(0) \rangle|^2 &= \frac{1}{(1 + |\alpha|^2)^2} \left(e^{-t/\tau_1} + |\alpha|^2 e^{-t/\tau_2} \right. \\
&\quad \left. + 2|\alpha| e^{-t(\tau_1+\tau_2)/2\tau_1\tau_2} \cos t(E_2 - E_1) \right). \quad (18)
\end{aligned}$$

This is what underlies e.g. neutrino oscillations. To emphasize that it is the same physics here, recall that

$$\sqrt{(k_1 + k_2)^2 - |\mathbf{k}_1 + \mathbf{k}_2|^2} = M/H|\tau_{12}|. \quad (19)$$

Defining a physical energy similar to eqn (16),

$$E_{12} = (k_1 + k_2)H|\tau_{12}|, \quad (20)$$

T_φ^A can be rewritten as

$$\begin{aligned}
T_\varphi^A &\sim \sqrt{\frac{M^2}{H^2 \tau_{12} \tau_{34}}} \cos \left[\frac{M}{H} \ln \frac{(E_{12} + M)\tau_{34}}{(E_{34} + M)\tau_{12}} \right] \\
&\sim \sqrt{\frac{M^2}{H^2 \tau_{12} \tau_{34}}} \cos \left[\frac{M}{H} \ln \frac{\tau_{34}}{\tau_{12}} \right. \\
&\quad \left. + \ln \left(1 + \frac{E_{12}}{M} \right) - \ln \left(1 + \frac{E_{34}}{M} \right) \right]
\end{aligned}$$

Approximating $\ln(1 + E/M) = E/M + \dots$ and transforming to cosmological time $\tau = -e^{-Ht}/H$,

$$\begin{aligned}
T_\varphi^A &\sim \sqrt{\frac{M^2}{H^2 \tau_{12} \tau_{34}}} \cos \left[M(t_{12} - t_{34}) + \frac{E_{12}}{H} - \frac{E_{34}}{H} \right] \\
&\quad + \text{permutations} \quad (21)
\end{aligned}$$

we recognize the familiar ΔE interference term with a new cosmological Δt term as well. For the specific case $k_1 + k_2 = k_3 + k_4$ the energy is conserved, making the vertex interaction time equal, and the oscillations disappear. This is also scale-invariant, $g_{\text{NL}}^A \sim T_\varphi^A / P_\varphi^3 \sim 1$. By combining such high-energy interactions with local ones, there would be an enhancement as seen in [33].

To see whether these characteristic oscillatory features are present in the total signal, we must also compute the next two diagrams. They are

$$\begin{aligned}
T_\varphi^B &= \frac{(-ig_1)^2}{(2\pi)^3} \int_{\tau_{\text{in}}}^0 d\tau_1 a(\tau_1)^4 \int_{\tau_{\text{in}}}^0 d\tau_2 a(\tau_2)^4 \times \\
&\quad [-iG_{\mathbf{k}_1}^R(0, \tau_1)] F_{\mathbf{k}_2}(0, \tau_1) [-i\mathcal{G}_{\mathbf{k}_1+\mathbf{k}_2}^R(\tau_1, \tau_2)] F_{\mathbf{k}_3}(\tau_2, 0) F_{\mathbf{k}_4}(\tau_2, 0) \\
&\quad + \text{permutations,} \\
T_\varphi^C &= \frac{(-ig_1)^2}{(2\pi)^3} \int_{\tau_{\text{in}}}^0 d\tau_1 a(\tau_1)^4 \int_{\tau_{\text{in}}}^0 d\tau_2 a(\tau_2)^4 [-iG_{\mathbf{k}_1}^R(0, \tau_1)] \times \\
&\quad F_{\mathbf{k}_2}(0, \tau_1) [-i\mathcal{G}_{\mathbf{k}_1+\mathbf{k}_2}^R(\tau_1, \tau_2)] [-iG_{\mathbf{k}_3}^A(\tau_2, 0)] [-iG_{\mathbf{k}_4}^A(\tau_2, 0)] \\
&\quad + \text{permutations.}
\end{aligned}$$

Computing their effects, one easily sees that

$$T_\varphi^B = T_\varphi^C = -\frac{1}{2}T_\varphi^A.$$

The leading H/M contribution therefore vanishes.

Loop High-Energy Corrections

Now turning to the loop corrections in Figure 8, the first is

$$\begin{aligned} T_\varphi^D &= \frac{(-i\lambda_1)^2}{(2\pi)^3} \int_{\tau_{\text{in}}}^0 d\tau_1 a(\tau_1)^4 \int_{\tau_{\text{in}}}^0 d\tau_2 a(\tau_2)^4 \times \\ &\int \frac{d^3\mathbf{q}}{(2\pi)^3} \left([-iG_{\mathbf{k}_1}^R(0, \tau_1)] F_{\mathbf{k}_2}(0, \tau_1) F_{\mathbf{q}}(\tau_1, \tau_2) \times \right. \\ &\left. \mathcal{F}_{\mathbf{k}_1+\mathbf{k}_2+\mathbf{q}}(\tau_1, \tau_2) [-iG_{\mathbf{k}_3}^A(\tau_2, 0)] F_{\mathbf{k}_4}(\tau_2, 0) + \text{perms.} \right) \\ &= \frac{\lambda_1^2 H^4}{2\pi^3 (k_1 k_2 k_3 k_4)^{3/2}} \times \\ &\int \frac{d^3\mathbf{q}}{(2\pi)^3} \left[\mathcal{B}_1(\mathbf{k}_1, \mathbf{k}_2, \mathbf{q}) \mathcal{B}_1^*(\mathbf{k}_3, \mathbf{k}_4, \mathbf{q}) + \text{c.c.} + \text{perms.} \right]. \end{aligned}$$

There is a rapidly-varying phase present completely analogous to (12),

$$\left(\frac{k_1 + k_2 + q + \sqrt{(k_1 + k_2 + q)^2 - |\mathbf{k}_1 + \mathbf{k}_2 + \mathbf{q}|^2}}{k_3 + k_4 + q + \sqrt{(k_3 + k_4 + q)^2 - |\mathbf{k}_3 + \mathbf{k}_4 + \mathbf{q}|^2}} \right)^{-iM/H}$$

As in the bispectrum loop integration, the integration over \mathbf{q} will only allow contributions near $k_1+k_2 = k_3+k_4$. Now defining variables appropriate to this case,

$$\begin{aligned} \kappa_{12} &\equiv k_1 + k_2 - (k_3 + k_4), \\ u^{-1} &\equiv -\sqrt{(k_1 + k_2 + q)^2 - |\mathbf{k}_1 + \mathbf{k}_2 + \mathbf{q}|^2}, \\ E &\equiv Mq|u|. \end{aligned}$$

Taking θ to be the angle between $k_{12} \equiv \mathbf{k}_1 + \mathbf{k}_2$ and \mathbf{q} , the (u, E) variables can be inverted to yield

$$\begin{aligned} q &= \frac{E}{M|u|}, \\ 1 - \cos\theta &= \frac{M|u|}{2k_{12}E} \left[|u|^{-2} - (k_1 + k_2)^2 + k_{12}^2 \right]. \end{aligned}$$

Just as in the bispectrum case, the integral transforms as

$$\int \frac{d^3\mathbf{q}}{(2\pi)^3} \rightarrow -\frac{1}{(2\pi)^2 M^2 k_{12}} \int \frac{du E dE}{u^5}. \quad (22)$$

The integrand transforms as

$$\mathcal{B}_1(\mathbf{k}_1, \mathbf{k}_2, \mathbf{q}) \mathcal{B}_1^*(\mathbf{k}_3, \mathbf{k}_4, \mathbf{q}) \rightarrow \frac{\pi |u|^4 M^2 e^{-i\frac{M}{H}\kappa_{12}u}}{16HE\sqrt{k_1 k_2 k_3 k_4}} + \mathcal{O}(\kappa_{12}).$$

The bounds are now

$$\begin{aligned} \frac{M|u| \left[|u|^{-2} + k_{12}^2 - (k_1 + k_2)^2 \right]}{2(k_1 + k_2 + k_{12})} &\leq E \leq \Lambda - M(k_1 + k_2)|u|, \\ |u_\pm| &= \frac{1}{(k_{12} + k_1 + k_2)^2} \times \\ &\left[\left(\frac{\Lambda}{M} \right) k_{12} \pm \sqrt{\left(\frac{\Lambda}{M} \right)^2 k_{12}^2 - (k_{12} + k_1 + k_2)^2} \right]. \end{aligned}$$

The energy integral is again trivial, and expanding near the extremum at $|u_0| = M/\Lambda(k_1 + k_2 + k_{12})$ the resultant integrand can be approximated as Gaussian:

$$\begin{aligned} |u|^{-1} \left[\Lambda - M(k_1 + k_2)|u| \right. \\ \left. - \frac{M|u| \left[|u|^{-2} + k_{12}^2 - (k_1 + k_2)^2 \right]}{2(k_1 + k_2 + k_{12})} \right] \\ \approx \frac{\Lambda^2(k_1 + k_2 + k_{12})}{2M} \times \\ \exp \left[-\frac{1}{2} \left(\frac{\Lambda}{M} \right)^2 (k_1 + k_2 + k_{12})^2 (u - u_0)^2 \right]. \end{aligned}$$

Now performing the integral over u ,

$$\begin{aligned} \int_{-\infty}^{\infty} du e^{-i\frac{M}{H}\kappa_{12}u - \frac{1}{2}\left(\frac{\Lambda}{M}\right)^2(k_1+k_2+k_{12})^2(u-u_0)^2} + \text{c.c.} \\ \approx \frac{\sqrt{2\pi}M}{\Lambda(k_1 + k_2 + k_{12})} e^{-i\frac{M}{H}\kappa_{12}u_0 - \frac{1}{2}\left(\frac{M^2\kappa_{12}}{H\Lambda(k_1+k_2+k_{12})}\right)^2} + \text{c.c.} \\ \approx \frac{4\pi H}{M} \delta(\kappa_{12}). \end{aligned}$$

The final answer is then

$$T_\varphi^D = \frac{\pi \lambda_1^2 H^4 \Lambda^2 (k_1 + k_2 + k_{12})}{(2\pi)^4 M^2 (k_1 k_2 k_3 k_4)^2 k_{12}} \delta(k_1 + k_2 - k_3 - k_4) + \text{perms.} \quad (23)$$

The $(\Lambda/M)^2$ can be absorbed into the bare coupling λ_1 . Unlike the tree-level trispectrum corrections, there is no H/M dependence in the magnitude of (23). Like the other high-energy diagrams calculated, it is scale-invariant.

The next diagram is similar,

$$\begin{aligned} T_\varphi^E &= \frac{(-i\lambda_1)^2}{(2\pi)^3} \int_{\tau_{\text{in}}}^0 d\tau_1 a(\tau_1)^4 \int_{\tau_{\text{in}}}^0 d\tau_2 a(\tau_2)^4 \times \\ &\int \frac{d^3\mathbf{q}}{(2\pi)^3} \left([-iG_{\mathbf{k}_1}^R(0, \tau_1)] F_{\mathbf{k}_2}(0, \tau_1) [-iG_{\mathbf{q}}^R(\tau_1, \tau_2)] \times \right. \\ &\left. [-iG_{\mathbf{k}_1+\mathbf{k}_2+\mathbf{q}}^R(\tau_1, \tau_2)] [-iG_{\mathbf{k}_3}^A(\tau_2, 0)] F_{\mathbf{k}_4}(\tau_2, 0) + \text{perms.} \right). \end{aligned}$$

It is easy to see that $T_\varphi^E = -\frac{1}{2}T_\varphi^D$. Using the formula for u_c in the \mathcal{B} 's, we assume that $k_1 + k_2 \geq k_3 + k_4$ to ensure $u_1 \geq u_2$.

Finally, T_φ^F and T_φ^G cancel, and T_φ^H and T_φ^I cancel.

Total Trispectrum

Taking advantage of the cancellations between several diagrams, the total trispectrum is

$$T_\varphi = (2\pi)^6 \delta^3(\mathbf{k}_1 - \mathbf{k}_2) \delta^3(\mathbf{k}_3 - \mathbf{k}_4) P_\varphi(k_1) P_\varphi(k_3) \\ + \text{permutations} + T_\varphi^{\text{self}} + T_\varphi^D + T_\varphi^E.$$

While oscillations arise at order H/M in individual diagrams, their cancellation means that no such feature appears in the final result.

CONCLUSION

We have computed the *generic* primordial bi- and trispectrum corrections in an inflating background due to high energy physics. The dominant physics arises from the New Physics Hypersurface where the cosmological blueshift can just create an on-shell heavy particle. As predicted [17–19], the bispectrum corrections peak near the elongated shape of momentum-triangle; here we derive this *ab initio*. The bispectrum otherwise contains no extraordinary features. The trispectrum has no leading order effect. Even though the interference effect of the effective mass-shell-time-difference for a pair of heavy particles, similar to neutrino oscillations, this cancels when all diagrams are taken into account.

Like that of the power spectrum, the magnitude of the bispectrum high-energy corrections are estimated to be of order H/M . For optimistic but not impossible values of $H/M \sim 0.01$ these corrections could possibly be measured by *Planck* [8] and other precision experiments in the near future. Also like the power spectrum, the leading corrections arising from the dynamical part of the effective action cancel and the dominant corrections arise entire from the density matrix.

We emphasize that we have only calculated the model-independent corrections. Specific models will no doubt produce very rich features and should be studied in more detail.

ACKNOWLEDGMENTS

We would like to thank F. Bouchet, J. Fergusson, E. Komatsu, and B. Wandelt for discussions. This research was supported in part by a VIDJ and a VICI Innovative Research Incentive Award from the Netherlands Organisation for Scientific Research (NWO), a van Gogh grant from the NWO, and the Dutch Foundation for Fundamental Research on Matter (FOM).

- [1] A. H. Guth, “The Inflationary Universe: A Possible Solution To The Horizon And Flatness Problems,” *Phys. Rev. D* **23**, 347 (1981).
- [2] A. D. Linde, “A New Inflationary Universe Scenario: A Possible Solution Of The Horizon, Flatness, Homogeneity, Isotropy And Primordial Monopole Problems,” *Phys. Lett. B* **108**, 389 (1982).
- [3] A. Albrecht and P. J. Steinhardt, “Cosmology For Grand Unified Theories With Radiatively Induced Symmetry Breaking,” *Phys. Rev. Lett.* **48**, 1220 (1982).
- [4] A. D. Linde, “Chaotic Inflation,” *Phys. Lett. B* **129**, 177 (1983).
- [5] R. H. Brandenberger, “Inflationary cosmology: Progress and problems,” arXiv:hep-ph/9910410.
- [6] B. Greene, K. Schalm, J. P. van der Schaar and G. Shiu, “Extracting new physics from the CMB,” *In the Proceedings of 22nd Texas Symposium on Relativistic Astrophysics at Stanford University, Stanford, California, 13-17 Dec 2004*, pp 0001 [arXiv:astro-ph/0503458].
- [7] E. Komatsu *et al.* [WMAP Collaboration], “Seven-Year Wilkinson Microwave Anisotropy Probe (WMAP) Observations: Cosmological Interpretation,” arXiv:1001.4538 [astro-ph.CO]; D. Larson *et al.* [WMAP Collaboration], “Seven-Year Wilkinson Microwave Anisotropy Probe (WMAP) Observations: Power Spectra and WMAP-Derived Parameters,” arXiv:1001.4635 [astro-ph.CO].
- [8] [Planck Collaboration], “Planck: The scientific programme,” arXiv:astro-ph/0604069.
- [9] “*Euclid: Mapping the geometry of the dark universe*”, Assessment Report by the ESA, December 2009.
- [10] D. Baumann, M. G. Jackson *et al.* [CMBPol Study Team Collaboration], “CMBPol Mission Concept Study: Probing Inflation with CMB Polarization,” *AIP Conf. Proc.* **1141**, 10-120 (2009). [arXiv:0811.3919 [astro-ph]]; D. Baumann *et al.* [CMBPol Study Team Collaboration], “CMBPol Mission Concept Study: A Mission to Map our Origins,” *AIP Conf. Proc.* **1141**, 3 (2009) [arXiv:0811.3911 [astro-ph]].
- [11] E. Komatsu *et al.*, “Non-Gaussianity as a Probe of the Physics of the Primordial Universe and the Astrophysics of the Low Redshift Universe,” arXiv:0902.4759 [astro-ph.CO].
- [12] A. P. S. Yadav and B. D. Wandelt, “Evidence of Primordial Non-Gaussianity ($f(\text{NL})$) in the Wilkinson Microwave Anisotropy Probe 3-Year Data at 2.8sigma,” *Phys. Rev. Lett.* **100**, 181301 (2008) [arXiv:0712.1148 [astro-ph]].
- [13] L. Senatore, K. M. Smith and M. Zaldarriaga, “Non-Gaussianities in Single Field Inflation and their Optimal Limits from the WMAP 5-year Data,” *JCAP* **1001**, 028 (2010) [arXiv:0905.3746 [astro-ph.CO]].
- [14] E. Komatsu and D. N. Spergel, “Acoustic signatures in the primary microwave background bispectrum,” *Phys. Rev. D* **63**, 063002 (2001) [arXiv:astro-ph/0005036].
- [15] P. Creminelli, “On non-Gaussianities in single-field inflation,” *JCAP* **0310**, 003 (2003) [arXiv:astro-ph/0306122].
- [16] M. Alishahiha, E. Silverstein and D. Tong, “DBI in the sky,” *Phys. Rev. D* **70**, 123505 (2004) [arXiv:hep-th/0404084].

- [17] R. Holman and A. J. Tolley, “Enhanced Non-Gaussianity from Excited Initial States,” *JCAP* **0805**, 001 (2008) [arXiv:0710.1302 [hep-th]].
- [18] P. D. Meerburg, J. P. van der Schaar and P. S. Corasaniti, “Signatures of Initial State Modifications on Bispectrum Statistics,” *JCAP* **0905**, 018 (2009) [arXiv:0901.4044 [hep-th]].
- [19] P. D. Meerburg, J. P. van der Schaar and M. G. Jackson, “Bispectrum signatures of a modified vacuum in single field inflation with a small speed of sound,” *JCAP* **1002**, 001 (2010) [arXiv:0910.4986 [hep-th]].
- [20] X. Chen, “Folded Resonant Non-Gaussianity in General Single Field Inflation,” *JCAP* **1012**, 003 (2010) [arXiv:1008.2485 [hep-th]].
- [21] J. Ganc, “Calculating the local-type fNL for slow-roll inflation with a non-vacuum initial state,” *Phys. Rev. D* **84**, 063514 (2011) [arXiv:1104.0244 [astro-ph.CO]].
- [22] D. Chialva, “Signatures of very high energy physics in the squeezed limit of the bispectrum from the field theoretical approach,” arXiv:1108.4203 [astro-ph.CO].
- [23] J. R. Fergusson, M. Liguori and E. P. S. Shellard, “The CMB Bispectrum,” arXiv:1006.1642 [astro-ph.CO].
- [24] M. G. Jackson and K. Schalm, “Model Independent Signatures of New Physics in the Inflationary Power Spectrum,” *Phys. Rev. Lett.* **108**, 111301 (2012) [arXiv:1007.0185 [hep-th]].
- [25] M. G. Jackson and K. Schalm, “Model-Independent Signatures of New Physics in Slow-Roll Inflation,” arXiv:1104.0887 [hep-th].
- [26] M. G. Jackson, “Integrating out Heavy Fields in Inflation,” arXiv:1203.3895 [hep-th].
- [27] E. Calzetta and B. L. Hu, “Nonequilibrium Quantum Fields: Closed Time Path Effective Action, Wigner Function and Boltzmann Equation,” *Phys. Rev. D* **37**, 2878 (1988).
- [28] T. S. Bunch and P. C. W. Davies, “Quantum Field Theory In De Sitter Space: Renormalization By Point Splitting,” *Proc. Roy. Soc. Lond. A* **360**, 117 (1978).
- [29] J. M. Maldacena, “Non-Gaussian features of primordial fluctuations in single field inflationary models,” *JHEP* **0305**, 013 (2003) [arXiv:astro-ph/0210603].
- [30] X. Chen, M. x. Huang, S. Kachru and G. Shiu, “Observational signatures and non-Gaussianities of general single field inflation,” *JCAP* **0701**, 002 (2007) [arXiv:hep-th/0605045].
- [31] E. Sefusatti, M. Liguori, A. P. S. Yadav, M. G. Jackson and E. Pajer, “Constraining Running Non-Gaussianity,” *JCAP* **0912**, 022 (2009) [arXiv:0906.0232 [astro-ph.CO]].
- [32] W. Hu, “Angular trispectrum of the CMB,” *Phys. Rev. D* **64**, 083005 (2001) [astro-ph/0105117].
- [33] I. Agullo, J. Navarro-Salas and L. Parker, “Enhanced local-type inflationary trispectrum from a non-vacuum initial state,” arXiv:1112.1581 [astro-ph.CO].
- [34] The fact that the interactions are tadpoles for χ is not an obstacle in applying our methods.